

Applied Mathematics and Nonlinear Sciences

<http://journals.up4sciences.org>

MHD mixed convection heat transfer over a non-linear slender elastic sheet with variable fluid properties

K. V. Prasad^{a†}, Hanumesh Vaidya^a and K. Vajravelu^b.

^aDepartment of Mathematics, VSK University, Vinayaka Nagar, Ballari 583 105, Karnataka, INDIA

^bDepartment of Mathematics, Department of Mechanical, Materials and Aerospace Engineering, University of Central Florida, Orlando, FL 32816, USA

Submission Info

Communicated by Juan L.G. Guirao

Received 22th March 2017

Accepted 31th August 2017

Available online 31th August 2017

Abstract

An analysis is presented for mixed convection and heat transfer in a viscous electrically conducting fluid flow at an impermeable stretching vertical sheet with variable thickness. The nonlinear equations that describe the fluid flow, and heat transfer processes have been solved using the Keller-box method. A limited parametric study is undertaken to determine the sensitivity and changes in the flow and temperature fields with respect to variations in the buoyancy parameter, the temperature dependent viscosity and thermal conductivity parameters, the plate velocity power index, and the Prandtl number which are presented in graphical and tabulated formats. To validate the results, comparisons are made with the available results in the literature for some special cases and the results are found to be in good agreement. The effects of embedded parameters on the dimensionless velocity profiles and temperature are examined through graphs. The variation of Local Nusselt number is also analysed. One of the important findings of our study is that the velocity distribution at a point near the plate decreases as the wall thickness parameter increases and hence the thickness of the boundary layer becomes thinner when $m < 1$. Further, the effect of the magnetic field is to reduce the fluid velocity and to increase the temperature field.

Keywords: Mixed convection, variable fluid properties, Keller-box method, flow and heat transfer, Variable thickness
AMS 2010 codes: 35Q79.

1 Introduction

The study of magneto hydrodynamic (MHD) flow and heat transfer has attracted numerous researchers due to its application to many technological and industrial processes, such as magnetic materials processing,

[†]Corresponding author.

Email address: prasadkv2007@gmail.com

purification of crude oil, magneto hydrodynamic electrical power generation, glass manufacturing, geophysics, and paper production, etc. Pavlov [1] used boundary-layer approximation theory to solve the problem of the flow of an electrically conducting fluid caused by a stretching elastic surface in the presence of a uniform magnetic field. Chakrabarti and Gupta [2] extended the work of Pavlov [1] and studied the flow evolution and heat transfer characteristics in flow over a stretching sheet with uniform suction. Applications of these results can be found in polymer technology and metallurgy. Watanabe [3] studied the characteristics of MHD boundary layer flow past a flat plate with a pressure gradient. Andersson [4] extended the work of Chakrabarti and Gupta [2] to a power law fluid while Chiam [5] obtained an accurate expression for the skin friction coefficient using Crocco's transformation for a power-law velocity distribution in a conducting fluid. Chamkha [6] considered the problem of hydro-magnetic three-dimensional free convection flow on a vertical porous stretching surface. Abel et al. [7] investigated the effect of a magnetic field on a non-Newtonian fluid flow and obtained solutions for different profiles and their asymptotic limits for large and small Prandtl numbers. Recently, Sheikholeslami et al [8] used a semi analytical method to obtain solutions for nanofluid flow and heat transfer between parallel plates subject to a time-dependent magnetic field. Watanabe [3] presented a theoretical study that sought to describe the behavior of an electrically conducting fluid past a semi-infinite flat plate subject to a transverse magnetic field. In many practical situations, the material moves in a quiescent fluid with the fluid flow induced by the motion of the solid material and by the thermal buoyancy. Therefore the resulting flow and the thermal fields are determined by these two mechanisms. It is well known that the buoyancy force stemming from the heating or cooling of the continuous stretching sheet alter the flow and the thermal fields and thereby heat transfer characteristics of the manufacturing processes. However, the significance and impact of the buoyancy force were not assessed in the studies reviewed above. Furthermore, the study of convection heat transfer around or past a sphere, a cone, and a wedge has practical applications. The heat flow around these objects has applications in fields that include spacecraft design and nuclear reactors, Ostrach [9] studied free-convection flow about a flat plate and obtained theoretical and experimental results for velocity and temperature distributions. (See for details Kothandaraman and Subramanyan [10]). A study of mixed convection along a moving surface was carried out by Moutsoglou and Chen [11]. Mixed convection heat transfer at a stretching sheet with variable temperature was investigated by Vajravelu [12]. Ishak et al. [13] analyzed the hydromagnetic effects to mixed convection flow near a vertical stretching sheet. Some relevant studies in this area have been reported by researchers including Ali and Al-Yousef [14], Nandkeolyar et al. [15], Mastroberardino [16], Srinivasacharya and Ram Reddy [17].

Renewed interest in the stretching sheet problem was sparked by a realization that some physical problems may be better modeled by a nonlinearly stretching sheet. Researchers who have reported the behaviour of fluid flow due to a nonlinear stretching sheet are Chaim [6], Prasad et al. [18], Ahmad et al. [19], Akyildiz et al. [20] and Kameswaran et al. [21]. Variable thickness of the sheet is useful in the mechanical, civil, marine and aeronautical structures and designs. The use of variable thickness helps to reduce the weight of structural elements and improve the utilization of the material. Sheets with variable thickness are often used in machine design, architecture, nuclear reactor technology, naval structures and acoustical components. With these industrial applications in mind, Lee [22] introduced the idea of variable thickness in theoretical studies. Fang et al. [23] studied the behaviour of boundary layer flow over a stretching sheet with variable thickness and explained the significant effects of the non-flatness of the sheet on the velocity and shear stress profiles by considering a special type of non-linear stretching $u_w(x) = U_0(x+b)^m$ for different values of m being b and U_0 constants. Khader et al. [24] extended the work of Fang et al. [23] and obtained the numerical solution for the slip velocity effect. Recently, Prasad et al. [25] and Vajravelu et al. [26], focused on heat transfer characteristics of fluid flow over a stretching sheet with variable thickness and power law velocity in the presence of a variable magnetic field.

Most of the studies above restricted their analysis to the hydromagnetic flow and heat transfer over a horizontal or a vertical plate and assumed the thermo-physical properties of the ambient fluid to be constant. However, it is known that these physical properties may change with temperature, especially the fluid viscosity and fluid thermal conductivity (Prasad et al. [18], Vajravelu et al. [27], Prasad et al. [28], and Hassanien [29]). For lubricating fluids, heat generated by internal friction and the corresponding rise in the temperature affects the physical

properties of the fluid, and the properties of the fluid can no longer be assumed to be constant. The increase in temperature leads to an increase in the transport processes including heat transfer at the wall. Therefore, to predict the flow and heat transfer rates, it is necessary to take into account the variable fluid properties. From the literature, we find no evidence of previous studies on the combined effects of variable fluid properties and mixed convection in flow over a slender stretching sheet with variable thickness.

The problem studied here extends the work of Prasad et al. [18] to the mixed convection flow with variable thickness. The coupled non-linear partial differential equations modeling the flow problem have been transformed to a system of coupled non-linear ordinary differential equations. These equations have been solved numerically using the Keller-box method, which is essentially a second order finite difference method. Computed numerical results for the flow and heat transfer characteristics are found to be in good agreement with experimental results in the literature (Fang et al. [23] and Khader et al. [24]). It is expected that the obtained results will not only provide useful information for industrial applications but would also serve to compliment and validate previous works.

2 Mathematical formulation

Consider a mixed convection boundary layer flow of a viscous incompressible electrically conducting fluid in the presence of a transverse magnetic field $B(x)$ past an impermeable stretching vertical heated sheet with variable thickness. The origin is located at the slit, through which the sheet (see Fig. 1) is drawn in the fluid.

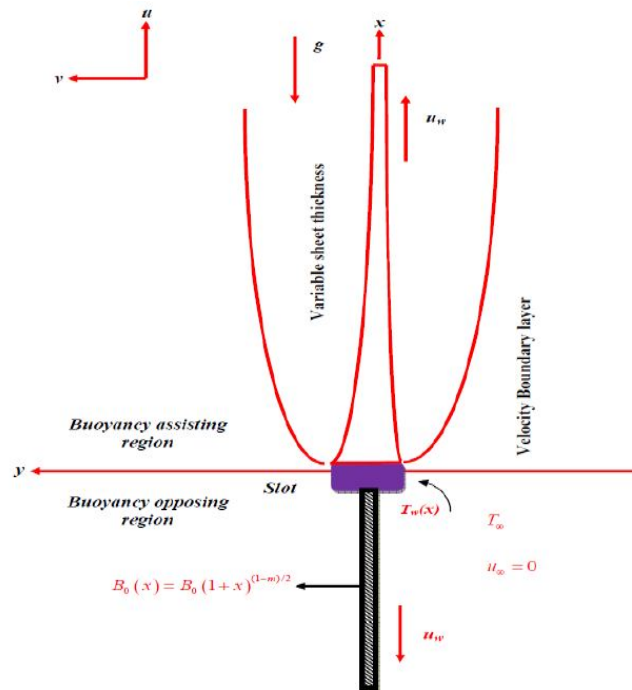


Fig.1 Schematic diagram of the stretching sheet with variable thickness model.

Two equal and opposite forces are applied impulsively along the x -axis so that the sheet is stretched, keeping the origin fixed. The stationary coordinate system has its origin located at the center of the sheet with the x -axis extending along the sheet, while the y -axis is measured normal to the surface of the sheet and is positive in the direction of the sheet to the fluid. We assume that the wall is impermeable ($V_w = 0$) and that the sheet is stretched with a velocity $U_w(x) = U_0(x + b)^m$ where U_0 is constant, b is a physical parameter related to stretching sheet and m is the velocity exponent parameter. The sheet is not flat and its thickness is defined

by $y = A(x + b)^{(1-m)/2}$, where the coefficient A is small so that the sheet is sufficiently thin, to avoid pressure gradient along the sheet ($\partial p / \partial x = 0$). For different applications, due to the acceleration or deceleration of the sheet, the thickness of the stretched sheet may decrease or increase with distance from the slot, which is dependent on the value of the velocity power index, m , and $m = 1$ represents a sheet of uniform thickness. For $m = 1$, the sheet is flat. The magnetic Reynolds number is assumed to be small so that the induced magnetic field is negligible. The viscous dissipation and Ohmic heating terms are not included in the energy equation since they are generally small. Under these assumptions and invoking the Boussinesq and boundary layer approximations, the governing equations for mass, momentum and energy for the model in the presence of temperature dependent fluid properties are (for details see Fang et al. [23] and Vajravelu [12])

$$u_x + v_y = 0,$$

$$\rho_\infty(uu_x + vv_y) = (\mu u_y)_y \pm g\beta(T - T_\infty) - \sigma B_0^2(x)u, \quad (1)$$

$$\rho_\infty c_p(uT_x + vT_y) = (k(T)T_y)_y, \quad (2)$$

where u and v are the fluid velocity components in the stream wise and cross-stream directions, respectively. The suffix denotes partial differentiation with respect to the independent variables, ρ_∞ is the constant fluid density, g is the acceleration due to gravity, β is the coefficient of thermal expansion, μ is the coefficient of viscosity which varies as an inverse function of temperature (for details see Vajravelu et al. [27] and Prasad et al. [28]) and is as follows:

$$\mu = \frac{\mu_\infty}{[1 + \gamma(T - T_\infty)]}, \text{ i.e., } \frac{1}{\mu} = a(T - T_r), \quad (3)$$

where $a = \frac{\gamma}{\mu_\infty}$ and $T_r = T_\infty - \frac{1}{\gamma}$. Here both a and T_r are constants whose values depend on both the reference state and the thermal properties of the fluid. In general, $a > 0$ corresponds to a liquid and $a < 0$ for gasses T is the temperature; T_∞ and μ_∞ are the constant ambient temperature and coefficient of viscosity respectively far from the sheet. The second term on the right hand side of Eq. (1) represents the influence of thermal buoyancy force on the flow field, with “+” and “-” sign referring to the buoyancy assisting and buoyancy opposing flow region, respectively. Fig. 1 provides the necessary information for such a flow field for a stretching vertical heated sheet with the upper half of the flow field being assisted and the lower half of the flow field being opposed by the buoyancy force. Also, σ is the electrical conductivity, $B_0^2(x) = B_0^2(x + b)^{m-1}$ is the magnetic field. This form of $B_0^2(x)$ has also been considered by several researchers when studying MHD flow problems (see Chaim [6] and Prasad et al. [18]) over a moving or fixed flat plate. C_p is the specific heat at constant pressure and $k(T)$ is the temperature-dependent thermal conductivity. We consider the temperature dependent thermal conductivity in the form (see Vajravelu et al. [27] and Prasad et al. [28])

$$k(T) = k_\infty \left(1 + \frac{\varepsilon}{\Delta T} (T - T_\infty)\right), \quad (4)$$

where $\Delta T = (T_w - T_\infty = \frac{C}{l}(x + b)^r$, T_w is the sheet temperature, C is a constant, l is the characteristic length, ε is the thermal conductivity parameter and k_∞ is thermal conductivity of the fluid away from the sheet, r is a wall temperature parameter (when $r > 0$, heat flows from the stretching sheet into the ambient medium and, when $r < 0$, the temperature gradient is positive and heat flows into the stretching sheet from the ambient medium). Substituting Eqs. (3) and (4) into Eqs. (1) and (2), we obtain

$$u \frac{\partial u}{\partial x} + v \frac{\partial u}{\partial y} = \frac{1}{\rho_\infty} \frac{\partial}{\partial y} \left(\frac{\mu_\infty}{1 + \gamma(T - T_\infty)} \frac{\partial u}{\partial y} \right) \pm \frac{g\beta(T - T_\infty)}{\rho_\infty} - \frac{\sigma B_0^2(x)}{\rho_\infty} u, \quad (5)$$

$$\rho_{\infty}c_p u \frac{\partial T}{\partial x} + \left(\rho_{\infty}c_p v - \frac{k_{\infty}\epsilon\partial T}{\Delta T\partial y} \right) \frac{\partial T}{\partial y} = \left(k_{\infty} \left(1 + \frac{\epsilon}{\Delta T}(T - T_{\infty}) \right) \right) \frac{\partial^2 T}{\partial y^2}. \tag{6}$$

The appropriate boundary conditions for the problem are

$$u(x, y) = U_w = U_0(x + b)^m, v(x, y) = 0, T(x, y) = T_w = \frac{C}{l}(x + b)^r + T_{\infty} \text{ at } y = A(x + b)^{\frac{1-m}{2}}, u(x, y) \rightarrow 0, T(x, y) \rightarrow T_{\infty} \text{ as } y \rightarrow \infty. \tag{7}$$

Now we transform the system of Eqs. (2.1)-(2.3) into a dimensionless form. To this end, let the dimensionless similarity variable be

$$\eta = y \sqrt{\frac{m+1}{2} \frac{U_0}{v_{\infty}} (x+b)^{\frac{m-1}{2}}}, \tag{8}$$

the stream function $\psi(x, y)$, and the dimensionless temperature distribution $\theta(\eta)$ be

$$\psi(x, y) = f(\eta) \sqrt{\frac{2}{m+1} U_0 v_{\infty} (x+b)^{\frac{m+1}{2}}}, \quad \theta(\eta) = \frac{(T - T_{\infty})}{(T_w - T_{\infty})}. \tag{9}$$

Using Eq. (9), the velocity components can be written as

$$u = U_w f'(\eta) \text{ and } v = -\sqrt{v_{\infty} \frac{m+1}{2} U_0 (x+b)^{\frac{m-1}{2}}} \left[f(\eta) + \eta f'(\eta) \left(\frac{m-1}{m+1} \right) \right] \tag{10}$$

Here the prime denotes differentiation with respect to η . In the present work, it is assumed $m > -1$ for the validity of the similarity variable. Using Eqs. (8)-(10) and Eqs. (5), (6) and (7), now reduce to

$$\left(\frac{f''}{(1 - \theta/\theta_r)} \right)' + f f'' - \frac{2m}{(m+1)} f'^2 - Mn f' + \lambda \theta = 0, \tag{11}$$

$$\left[(1 + \epsilon \theta) \theta' \right]' + Pr \left(f \theta' - \frac{2r}{m+1} \theta f' \right) = 0,$$

The non-dimensional parameters θ_r, Mn, λ and Pr are respectively, the fluid viscosity parameter, magnetic parameter, buoyancy or mixed convection parameter, the Prandtl number. These parameters are defined

$$\theta_r = \frac{T_r - T_{\infty}}{T_w - T_{\infty}} = -\frac{1}{\gamma(T_w - T_{\infty})}, Mn = \frac{2\sigma B_0^2}{\rho_{\infty} U_0 (1+m)}, \lambda = \frac{\pm g \beta C}{l U_0^2} \text{ and } Pr = \frac{v_{\infty}}{\alpha_{\infty}}.$$

The mixed convection parameter λ is independent of x if $r = 2m - 1$. Thus, the similarity solutions are obtained under this limitation when $\lambda \neq 0$. We note that when $r = 2m - 1$, λ is a constant, with $\lambda > 0$ and $\lambda < 0$ corresponding to assisting flow and opposing flow, respectively, while $\lambda = 0$, i.e., $(T_w = T_{\infty})$ represents the case when the buoyancy force is absent (that is, pure forced convection flow). On other hand, if λ is of a significantly greater order of magnitude than unity, the buoyancy forces will be dominant and the flow will essentially be free convective. Hence, mixed convective flow exists when $\lambda = O(1)$. Under the limitation $r = 2m - 1$, Eq. (11) becomes

$$\left[(1 + \epsilon \theta) \theta' \right]' + Pr \left(f \epsilon' - \frac{2(2m-1)}{m+1} \theta f' \right) = 0,$$

and the corresponding boundary conditions are ($m \neq -1$)

$$f(\alpha) = \alpha \frac{1-m}{1+m}, f'(\alpha) = 1, \theta(\alpha) = 1, \theta(\infty) = 0, f'(\infty) = 0.$$

The value of θ_r is determined by the viscosity of the fluid and the operating temperature difference. If θ_r is large then $(T_\infty - T_w)$ is small and the effects of variable viscosity can be neglected. On other hand, for smaller values of θ_r , the fluid viscosity changes markedly with temperature. Also, bearing in mind that the liquid viscosity varies differently with temperature compared to a gas, it is important to note that θ_r is negative for liquids and positive for gasses. Further, the viscosity of a fluid usually decreases with an increase in the temperature. Here $\alpha = A\sqrt{\frac{m+1}{2} \frac{U_\infty}{\nu_\infty}}$ is the wall thickness parameter and $\eta = \alpha = A\sqrt{\frac{m+1}{2} \frac{U_\infty}{\nu_\infty}}$ indicates the plate surface. In order to facilitate simulations, we define $f(\xi) = f(\eta - \alpha)$ and $\theta(\xi) = \theta(\eta - \alpha)$. The similarity equations become

$$\left(\frac{f''}{1 - \frac{\theta}{\theta_r}}\right)' + f f'' - \frac{2m}{m+1} f'^2 - Mn f' + \lambda \theta = 0, \tag{12}$$

$$\left[(1 + \varepsilon \theta) \theta'\right]' + Pr \left(f \theta' - \frac{2(2m-1)}{m+1} \theta f'\right) = 0, \tag{13}$$

and the corresponding boundary conditions are ($m \neq 1$)

$$\begin{aligned} f(0) = \alpha = \alpha \frac{1-m}{1+m}, f'(0) = 1, \theta(0) = 1, \\ \lim_{\xi \rightarrow \infty} f'(\xi) = \lim_{\xi \rightarrow \infty} \theta(\xi) = 0, \end{aligned} \tag{14}$$

where the prime denotes the differentiation with respect to ξ . Based on the variable transformation, the solution domain is fixed from 0 to ∞ . The shear stress and wall temperature gradient respectively become $f''(\alpha) = f''(0)$ and $\theta'(\alpha) = \theta'(0)$.

For practical purposes, the important physical quantities of interest are the local skin friction C_{f_x} and the local Nusselt number Nu_x , defined as:

$$\begin{aligned} C_{f_x} &= \frac{2\nu_\infty (u_y)_{y=A(x+b)^{\frac{1-m}{2}}}}{U_w^2} = 2\sqrt{\frac{m+1}{2}} (Re_x)^{-1/2} f''(0), \\ Nu_x &= \frac{(x+b) (T_y)_{y=A(x+b)^{\frac{1-m}{2}}}}{T_w - T_\infty} = -\sqrt{\frac{m+1}{2}} (Re)^{1/2} \theta'(0), \end{aligned}$$

where $Re_x = \frac{U_w(x+b)}{\nu_\infty}$ is the local Reynolds number.

3 Exact Solutions for the some special cases

Here we present some exact solutions for certain special cases. Such solutions are useful and serve as a baseline for comparison with the solutions obtained via other numerical / analytical schemes. In the case of constant fluid properties, the absence of a magnetic field and in the presence of buoyancy parameter with flat plate ($m = 1, b = 0$), Eqs. (12) and (13) reduce to those of Vajravelu [12]; while in the absence of variable fluid properties, buoyancy parameter and magnetic parameter, Eq. (12) reduce to those of Fang et al. [23].

Constant fluid properties without fluid buoyancy ($\theta_r \rightarrow \infty, \varepsilon = 0, \lambda = 0$ and $m = 1, b = 0$)

In the limiting case, $\theta_r \rightarrow \infty, \lambda = 0$ and $m = 1$ the boundary layer flow and heat transfer problem corresponds to the flat plate problem. The solution for the velocity in the presence of the magnetic field is $f(\xi) = \frac{1-e^{-\xi\beta}}{\beta}$ and $f'(\xi) = e^{-\xi\beta}$, where $\beta = \sqrt{1+Mn}$ and the solution for the temperature field can be written as a two parameter solution in terms of Confluent hypergeometric series, namely, Kummer's function, ϕ , as:

$$\theta(\eta) = e^{\frac{Pr}{\beta}\eta} \frac{\phi(a_1, b_1, z)}{\phi(a_1, b_1, -a_0)}, \text{ where } a_0 = \frac{Pr}{\beta^2}, a_1 = a_0 - r, b_1 = 1 + a_0, z = -a_0 e^{-\beta\eta}.$$

Constant fluid properties no buoyancy force, magnetic field, heat transfer and in the presence of variable thickness ($\theta_r \rightarrow \infty, \varepsilon = 0, \lambda = \text{Mn} = 0.0, m \neq 1, r = 0$)

When $m = \frac{-1}{3}$, Eq. (12) becomes $f''' + ff'' + f'^2 = 0$ with the boundary conditions as $f(0) = 2\alpha, f'(0) = 1, f'(\infty) = 0$. Hence, the solution is

$$f(\xi) = \sqrt{2 + 4\alpha^2} \tanh \left[\frac{\sqrt{2 + 4\alpha^2}}{2} \xi + \tanh^{-1} \left(\frac{2\alpha}{\sqrt{2 + 4\alpha^2}} \right) \right].$$

When $m = \frac{-1}{2}$, Eq. (12) becomes $f''' + ff'' + f'^2 = 0$ with the boundary conditions as

$f(0) = 3\alpha, f'(0) = 1, f'(\infty) = 0$. This equation is equivalent to $\frac{1}{f} \frac{d}{d\xi} \left[f^{3/2} \frac{d}{d\xi} \left(f^{-1/2} f' + \frac{2}{3} f^{3/2} \right) \right] = 0$ with solution

$$\eta + D = \frac{1}{2d^2} \log \left[\frac{f + d\sqrt{f} + d^2}{(d - \sqrt{f})^2} \right] + \frac{\sqrt{3}}{d^2} \tan^{-1} \left(\frac{2\sqrt{f} + d}{d\sqrt{3}} \right),$$

where $d = \left[(3\alpha)^{3/2} + \frac{3}{2\sqrt{3}\alpha} \right]^{1/3}$ and $D = \frac{1}{2d^2} \log \left[\frac{3\alpha + d\sqrt{3}\alpha + d^2}{(d - \sqrt{3}\alpha)^2} \right] + \frac{\sqrt{3}}{d^2} \tan^{-1} \left(\frac{2\sqrt{3}\alpha + d}{d\sqrt{3}} \right)$. Since the system of equations (12) and (13) with conditions (14) has no exact analytic solution they are solved numerically via a second order finite difference scheme.

4 Numerical procedure

Eqs. (12) and (13) are highly non-linear, coupled ordinary differential equations of third-order in $f(\xi)$, second-order $\theta(\xi)$ respectively. The system of equations subject to the boundary conditions (14) was solved numerically by an efficient finite difference scheme, namely the Keller-Box method (for details see Keller [30], Vajravelu and Prasad [31]). The numerical solutions are obtained in the following four steps:

- Reduce equations (12) and (13) to a system of first-order equations.
- Write the difference equations using central differences.
- Linearize the algebraic equations by Newton’s method, and write them in matrix-vector form.
- Solve the linear system by the block tri-diagonal elimination technique.

For numerical calculations, a uniform step size of $\Delta\eta = 0.01$ is found to be satisfactory and the solutions are obtained with an error tolerance of 10^{-6} . In order to validate the method used in this study and to judge the accuracy of the present analysis, comparison of the skin friction and the wall temperature gradient are made with the previously published results of Fang et al. [23], Khader and Megahed [24] for several special cases in which some thermo physical fluid properties are neglected. The results are found to be in excellent agreement and are shown in Tables 1 and 2.

5 Results and discussion

In order to get a clear insight of the physical problem, numerical computations have been carried out using the Keller-box method for different values of pertinent parameters such as the fluid viscosity parameter θ_r , the mixed convection parameter λ , the thermal conductivity parameter ε , the velocity power index parameter m , and the Prandtl number Pr. Analytical solutions have been obtained for the special case when $\theta_r \rightarrow \infty, m = 1, \lambda = 0$, and $\text{Mn} = 0$. We present the numerical results graphically for the horizontal velocity profile f'

with ξ and the temperature profile θ with ξ for different parameter values in Figs. 2 – 3. We observe that both f' and θ decrease asymptotically to zero with the distance from the boundary. The computed numerical values for the skin friction $f''(0)$ and the wall temperature gradient $\theta'(0)$ are given in Table 3.

Figs. 2(a) - 2(b) give a qualitative representation of the horizontal velocity f' for increasing values of α . Fig. 2(a) depicts the effect of λ on f' . The presence of thermal buoyancy effects is indicated by a finite value of λ ($\lambda \neq 0$). It is observed that an increase in the value of λ leads to an increase in f' . Physically $\lambda > 0$ implies heating of the fluid or cooling of the surface, $\lambda < 0$ suggests cooling of the fluid or heating of the surface, and $\lambda = 0$ corresponds to the absence of the mixed convection. An increase in λ means an increase in the temperature difference ($T_w - T_\infty$) which leads to an enhancement in f' due to the enhanced convection, and thus an increase in the momentum boundary layer thickness. Fig. 2(b) represents the effect of increasing θ_r on the velocity f' . The velocity decreases with increasing θ_r and as $\theta_r \rightarrow 0$ the momentum boundary layer thickness decreases. The velocity distribution is linear in shape for higher values of α . This is due to the fact that for a given fluid, when θ_r is smaller, higher is the temperature difference between the wall and the ambient fluid. The results clearly demonstrates that θ_r is the indicator of the variable fluid viscosity with temperature which has a substantial effect on the velocity component f' and hence on the skin friction. The effect of α on f' for zero and non zero values of m is demonstrated in Fig. 2(c). It shows that the velocity profile decreases with an increase in the value of α , this shows that the momentum boundary layer thickness becomes thinner as α increases. This phenomenon is even true for zero and negative value of m . The effect of m is to enhance the velocity profile which in turn increases the boundary layer thickness. Fig. 2(d) explains the effect of α on f' for different values of Mn. It is obvious that the presence of a magnetic field presents a higher constraint to the fluid flow, which reduces the fluid velocity and hence induces an increase in the absolute value of the velocity gradient at the surface. The magnetic field opposes the transport phenomena. This is due to the fact that with the increasing value of Mn, the Lorentz force associated with the magnetic field increases and it produces more resistance to the transport phenomena. The comparison of Fig. 2(c) and Fig. 2(d) reveals the significant effect of m (for $m < 0, m = 0$ and $m > 0$) on flow pattern. For negative values of m , the sheet is shrinking along the axis and if this is prominent then the fluid moves from upward region to downward region and further to its original upward region. This momentum transfer accelerates the fluid particle at the downward region. This significant change in the velocity can also be seen for positive values of m , the stretching sheet case. This trend is true for the temperature distribution also.

In Figs. 3(a)-3(e) the numerical results for the temperature distribution θ for several sets of values of the governing parameters are presented. Fig. 3(a) illustrates the effect of λ on θ for increasing values of α . With the increase in λ , temperature field is suppressed and consequently thermal boundary layer thickness becomes thinner and as a result rate of heat transfer from the plate increases, this is due to buoyancy force. Fig. 3(b) elucidates the effect of θ_r on θ for different values of α . From the graphical representation, we see that the effect of increasing value of θ_r is to enhance the temperature. This is because of the fact that an increase in θ_r results in an increase in the thermal boundary layer thickness. Fig. 3(c) exhibits the nature of temperature field for the variation of α for different values of m . Increase in α is to reduce the temperature distribution and thermal boundary layer becomes thinner for higher values of α . Fig. 3(d) exhibits the effect of α on θ for increasing values of Mn. As α increases the temperature profile increases. This can be observed even for the increasing values of Mn. As explained above, the transverse magnetic field gives rise to a resistive Lorentz force in the electrically conducting fluid. The fluid experiences a resistance due to increasing friction between its layers and thus increases the fluid temperature. The effect of Pr on θ is exhibited in Fig. 3(e) for zero and nonzero values of ε . Temperature is found to decrease with increasing Pr. An increase in the Pr reduces the thermal boundary layer thickness. Pr signifies the ratio of momentum diffusivity to thermal diffusivity. Fluids with lower Pr possess higher thermal conductivities and thicker thermal boundary layer structures so that heat can diffuse from the wall faster than higher Pr fluids thinner boundary layers. It can be observed from the profiles that, there is a prominent fall in the curve for Pr = 10 when compared to Pr = 1.0 which is in clear agreement with experimental results that thermal boundary layer thickness decreases with an increase of

Prandtl number (Chen [33], Ali [34]). Hence, Pr can control the rate of cooling in conducting flows. Further it is quite evident from the graph that the fluid temperature is found to increase with increasing values of ε which leads to a fall in the rate of heat transfer from the flow to the surface. This is due to the fact that the assumption of temperature dependent thermal conductivity suggests the reduction in the magnitude of the transverse velocity by a quantity $\partial k(T)/\partial y$ which can be located in Eq. (6). Therefore, the rate of cooling is much faster for the coolant material having small thermal conductivity parameter.

The effects of the physical parameters on the skin friction $f''(0)$ and the wall-temperature gradient $\theta'(0)$ are tabulated in Table 3. It is observed that for an increasing values of λ there is an increase in $f''(0)$ whereas decrease in $\theta'(0)$ and exactly opposite in the case of θ_r . It is also noticed that the effect of m and Mn is to decrease in both $f''(0)$ and $\theta'(0)$. Increasing Pr decreases $\theta'(0)$ and is reverse for increasing values of ε . Further, it is interesting to notice that for shrinking sheet case, there is a decrease in both $f''(0)$ and $\theta'(0)$ for increasing values of α , where as an opposite trend is observed for stretching sheet case.

Nomenclature

| | |
|------------|--|
| a | Constant in Eq. (3) |
| T | Temperature (K) |
| T_r | Constant in Eq. (3) |
| T_w | Temperature of the plate (K) |
| T_∞ | Ambient temperature (K) |
| ΔT | Temperature difference (K) |
| b | Constant in Eq. (7) known as stretching rate $b > 0$ |
| B_0 | Uniform magnetic field (Tesla) |
| r | Wall temperature parameter |
| C_p | Specific heat at constant pressure (J/kgK) |
| C_f | Skin friction |
| f | Dimensionless stream function |
| $K(T)$ | Temperature dependent thermal conductivity (W/mK) |
| K_∞ | Thermal conductivity of the fluid far away from the sheet (W/mK) |
| m | Velocity exponent parameter |
| Mn | Magnetic parameter |
| Nu_x | Nusselt number |
| Pr | Prandtl number |
| Re_x | Local Reynolds number |
| Sh_x | Sherwood number |
| u, v | Velocity components in the x and y directions (m/s) |
| $U_w(x)$ | Stretching velocity (m/s) |
| U_0 | Reference velocity (m/s) |
| x, y | Cartesian coordinates (m) |

Greek symbols

| | |
|---------------|---|
| α | Wall thickness parameter |
| λ | Buoyancy or mixed convection parameter |
| σ | Electric conductivity |
| ε | Constant in (2.5) known a variable thermal conductivity parameter |
| β | Thermal expansion coefficient |
| γ | Constant defined in equation (2.4) |
| ν_∞ | Kinematic viscosity away from the sheet (kg/m ³) |
| ρ | Density (kg/m ³) |
| ρ_∞ | Thermal conductivity of the fluid far away from the sheet (W/m K) |
| η, ξ | Similarity variables |
| θ | Dimensionless temperature |
| θ_r | Fluid viscosity parameter, constant in equation (2.12) |
| μ | Dynamic Viscosity (Pa s) |
| μ_∞ | Constant value of dynamic viscosity (Pa s) |
| ψ | Stream function |
| ϕ | Kummers' function |

Subscripts

| | |
|----------|-----------------------|
| ∞ | Condition at infinity |
| w | Condition at the wall |

Table 1: Comparison of skin friction $-f''(0)$ when for different values of m and α with $\theta_r \rightarrow \infty, m = 0, \varepsilon = 0.0, Mn = 0.0, \lambda = 0.0$.

| α | m | Fang et al. [23] By shooting method | Khader and Megahed [24] when Slip velocity parameter $\lambda=0$ By Chebyshev spectral method | Present Results |
|----------|------|-------------------------------------|---|-----------------|
| 0.5 | 10 | 1.0603 | 1.0603 | 1.060309 |
| | 9 | 1.0589 | 1.0588 | 1.058812 |
| | 7 | 1.0550 | 1.0551 | 1.055122 |
| | 5 | 1.0486 | 1.0486 | 1.048615 |
| | 3 | 1.0359 | 1.0358 | 1.035805 |
| | 2 | 1.0234 | 1.0234 | 1.023424 |
| | 1 | 1.0 | 1.0 | 1.0 |
| | 0.5 | 0.9799 | 0.9798 | 0.979848 |
| | 0 | 0.9576 | 0.9577 | 0.957727 |
| | -1/2 | 1.1667 | 1.1666 | 1.166666 |
| 0.25 | 10 | 1.1433 | 1.1433 | 1.143309 |
| | 9 | 1.1404 | 1.1404 | 1.140481 |
| | 7 | 1.1323 | 1.1323 | 1.132332 |
| | 5 | 1.1186 | 1.1186 | 1.118662 |
| | 3 | 1.0905 | 1.0904 | 1.090409 |
| | 1 | 1.0 | 1.0 | 1.0 |
| | 0.5 | 0.9338 | 0.9337 | 0.933770 |
| | 0 | 0.7843 | 0.7843 | 0.784309 |
| | -1/3 | 0.5000 | 0.5000 | 0.500000 |
| | -1/2 | 0.0833 | 0.08322 | 0.0832227 |

Table 2 Comparison of wall temperature gradient $\theta'(0)$ for different values of Prandtl number and magnetic parameter when $Mn = 0.0, \varepsilon = 0.0, \lambda = 0$, and $m = 1.0$.

| Pr | Present results | Grubka & Bobba [32] | Chen [33] | Ali [34] |
|-------|-----------------|---------------------|-----------|----------|
| 0.01 | -0.01017936 | -0.0099 | 0.0091 | - |
| 0.72 | -0.4631462 | -0.4631 | -0.46315 | -0.4617 |
| 1.0 | -0.5826707 | -0.5820 | -0.58199 | -0.5801 |
| 3.0 | -1.16517091 | -1.1652 | -1.16523 | -1.1599 |
| 5.0 | -1.56800866 | - | - | - |
| 10.0 | -2.308029 | -2.3080 | -2.30796 | -2.2960 |
| 100.0 | -7.769667 | -7.7657 | - | - |

Table 3: Variation of skin friction $f''(0)$ and wall-temperature gradient $\theta'(0)$ for different values of physical parameters.

| m | Mn | θ_r | Pr | ϵ | λ | $\alpha = 0.0$ | | $\alpha = 0.1$ | | $\alpha = 0.2$ | |
|-----------|----------|------------|-----|------------|------------|----------------|--------------|----------------|--------------|----------------|--------------|
| | | | | | | $f''(0)$ | $\theta'(0)$ | $f''(0)$ | $\theta'(0)$ | $f''(0)$ | $\theta'(0)$ |
| 2.0 | 0.1 | -5.0 | 1.0 | 0.1 | -5.0 | -1.545068 | -1.080793 | -1.522204 | -1.068792 | -1.499637 | -1.057054 |
| | | | | | 0.0 | -1.335278 | -1.146790 | -1.331519 | -1.134678 | -1.310604 | -1.122755 |
| | | | | | 0.5 | -1.185849 | -1.189561 | -1.165799 | -1.177318 | -1.146117 | -1.165239 |
| | | | | | 1.0 | -1.031486 | -1.222858 | -1.012449 | -1.210512 | -0.993795 | -1.198313 |
| 5.0 | 0.5 | -5.0 | 1.0 | 0.0 | -1.353883 | -1.530281 | -1.322420 | -1.502237 | -1.291802 | -1.474429 | |
| | | | | 0.1 | -1.352389 | -1.380212 | -1.320975 | -1.356161 | -1.290407 | -1.332783 | |
| | | | | 0.2 | -1.351008 | -1.262758 | -1.319643 | -1.242086 | -1.289123 | -1.222008 | |
| 5.0 | 0.5 | -5.0 | 0.1 | 1.0 | -1.353871 | -1.383738 | -1.320976 | -1.135616 | -1.290407 | -1.332783 | |
| | | | | 2.0 | -1.361864 | -2.092309 | -1.330033 | -2.037640 | -1.290407 | -1.984734 | |
| | | | | 5.0 | -1.371232 | -3.507749 | -1.334456 | -3.362246 | -1.307821 | -3.223160 | |
| | | | | 10.0 | -1.376316 | -5.101436 | -1.344081 | -4.806734 | -1.312650 | -4.529388 | |
| λ | Mn | θ_r | Pr | ϵ | α | m = -0.2 | | m = 0.0 | | m = 5.0 | |
| | | | | | | $f''(0)$ | $\theta'(0)$ | $f''(0)$ | $\theta'(0)$ | $f''(0)$ | $\theta'(0)$ |
| 0.1 | 0.0 | -5.0 | 1.0 | 0.1 | 0.0 | -0.227799 | 5.478141 | -0.631212 | 0.880672 | -1.376995 | -1.399540 |
| | | | | | 0.1 | -0.409797 | 3.568688 | -0.718014 | 0.679241 | -1.336629 | -1.376940 |
| | | | | | 0.2 | -0.593180 | 2.335793 | -0.808435 | 0.500008 | -1.297614 | -1.354864 |
| | | | | | 0.3 | -0.775887 | 1.545657 | -0.902260 | 0.337709 | -1.259952 | -1.333293 |
| | | | | | 0.5 | -1.141195 | 0.598557 | -1.099277 | 0.049424 | -1.188558 | -1.291576 |
| | | | | | 0.75 | -1.603216 | -0.121641 | -1.360758 | -0.266291 | -1.106376 | -1.241904 |
| λ | α | θ_r | Pr | ϵ | m | Mn = 0.0 | | Mn = 0.25 | | | |
| | | | | | | $f''(0)$ | $\theta'(0)$ | $f''(0)$ | $\theta'(0)$ | | |
| 0.1 | 0.0 | -5.0 | 1.0 | 0.1 | -0.2 | -0.248745 | 4.692819 | -0.548033 | 3.405338 | | |
| | | | | | -0.1 | -0.484413 | 1.895248 | -0.725686 | 1.517615 | | |
| | | | | | 0.0 | -0.640512 | 0.806492 | -0.849481 | 0.688922 | | |
| | | | | | 1.0 | -1.134166 | -0.889315 | -1.275859 | -0.858419 | | |
| | | | | | 5.0 | -1.375488 | -1.399645 | -1.496541 | -1.367532 | | |
| | | | | | 10.0 | -1.426228 | -1.494909 | -1.543140 | -1.464027 | | |
| λ | α | m | Pr | ϵ | θ_r | $\alpha = 0.0$ | | $\alpha = 0.5$ | | | |
| | | | | | | $f''(0)$ | $\theta'(0)$ | $f''(0)$ | $\theta'(0)$ | | |
| 0.1 | 0.0 | 2.0 | 1.0 | 0.1 | -10.0 | -1.212481 | -1.169201 | -1.123290 | -1.109093 | | |
| | | | | | -5.0 | -1.312789 | -1.152769 | -1.211471 | -1.094139 | | |
| | | | | | -3.0 | -1.435761 | -1.132209 | -1.317998 | -1.075621 | | |
| | | | | | -2.0 | -1.576301 | -1.108233 | -1.437581 | -1.054299 | | |

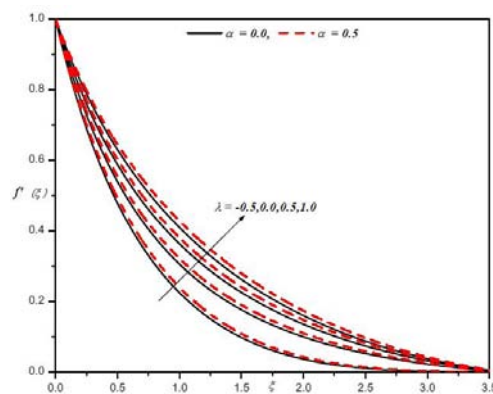


Fig.2(a): Horizontal velocity profiles for different values of λ and α with $Pr = 1.0, \epsilon = 0.1, Mn = 0.1, m = 2.0, \theta_r = -5.0$.

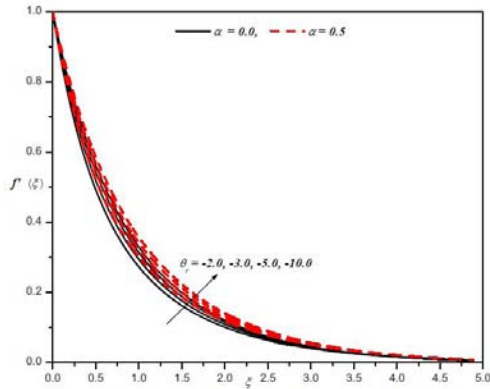


Fig.2(b): Horizontal velocity profiles for different values of θ and α with $\lambda = 0.1, Pr = 1.0, Mn = 0.1, m = 2.0, \epsilon = 0.1$.

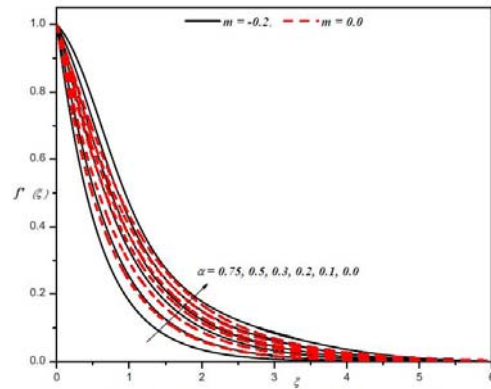


Fig.2(c): Horizontal velocity profiles for different values of α and m with $Pr = 1.0, \epsilon = 0.1, Mn = 0.0, \theta = -5.0, \lambda = 0.1$.

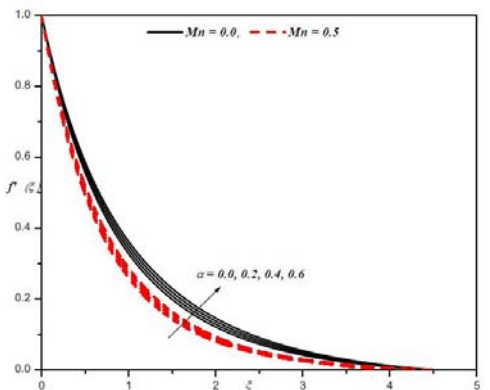


Fig.2(d): Horizontal velocity profiles for different values of α and Mn with $\theta = -5.0, \lambda = 0.1, \epsilon = 0.1, m = 2.0, Pr = 1.0$.

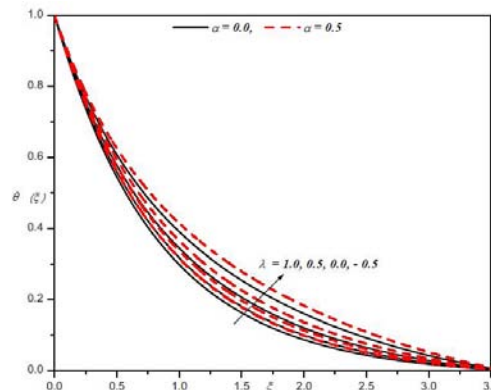


Fig.3(a): Temperature profiles for different values of λ and α when $Pr = 1.0, \epsilon = 0.1, Mn = 0.1, m = 2.0, \theta = -5.0$.

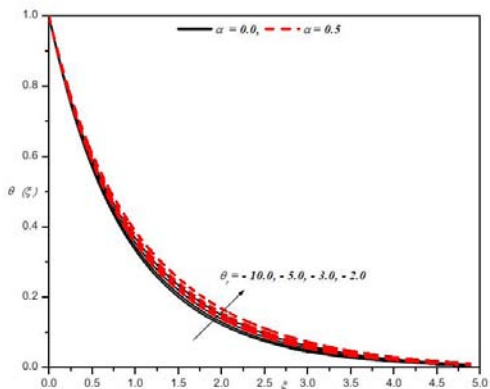


Fig.3(b): Temperature profiles for different values of θ and α with $\lambda = 0.1, Mn = 0.1, m = 2.0, \epsilon = 0.1, Pr = 1.0$.

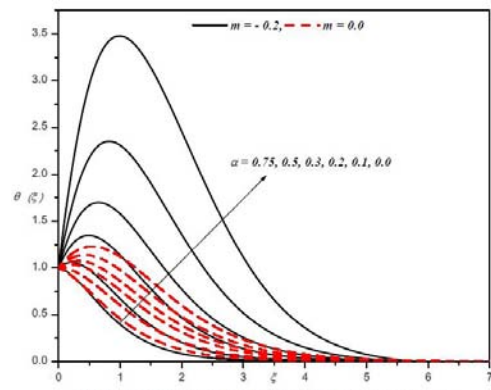


Fig.3(c): Temperature profiles for different values of m and α with $Pr = 1.0, \epsilon = 0.1, \lambda = 0.1, Mn = 0.0, \theta = -5.0$.

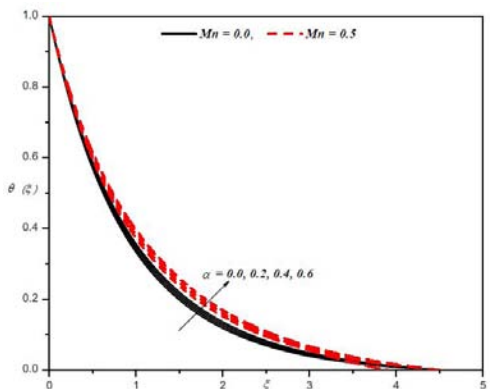


Fig.3(d): Temperature profiles for different values of α and Mn with $\theta = -5.0, \lambda = 0.1, \epsilon = 0.1, m = 2.0, Pr = 1.0$.

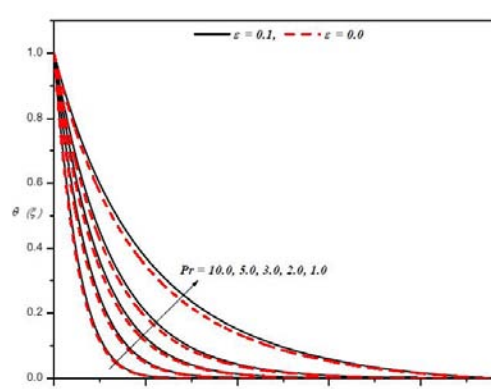


Fig.3(e): Temperature profiles for different values of Pr and ϵ with $\alpha = 0.5, Mn = 0.2, \theta = -5.0, m = 2.0, \lambda = 0.1$.

6 Conclusion

The numerical results indicate that the effect of increasing the mixed convection parameter is to increase the momentum boundary layer thickness whereas to decrease the thermal boundary layer thickness. Meanwhile, the dimensionless velocity distribution at a point near the plate decreases as the wall thickness parameter increases and hence the thickness of the boundary layer becomes thinner when $m < 1$. Further, the effect of the magnetic field is to reduce the fluid velocity and to increase the temperature field.

The rate of heat transfer increases with increasing magnetic parameter and the Prandtl numbers. Hence, the effect of Prandtl number is to decrease the thermal boundary layer thickness and the wall-temperature gradient. In addition to this, the effect of the variable thermal conductivity parameter is to enhance the temperature field.

References

- [1] K. B. Pavlov, (1974), *Magnetohydrodynamic flow of an incompressible viscous fluid caused by deformation of a plane surface*, Magnetohydrodynamics, 10, No 4, 507-510. doi [10.22364/mhd](https://doi.org/10.22364/mhd)
- [2] A. Chakrabarti and A. S. Gupta, (1979), *Hydromagnetic flow and heat transfer over a stretching sheet*, Quarterly of Applied Mathematics, 37, No 1, 73-78.
- [3] T. Watanabe, (1978), *Magnetohydrodynamic Stability of Boundary Layers along a Flat Plate in the Presence of a Transverse Magnetic Field*, ZAMM - Journal of Applied Mathematics and Mechanics, 58, No 12, 555-560. doi [10.1002/zamm.19780581205](https://doi.org/10.1002/zamm.19780581205)
- [4] H.I. Andersson, K.H. Bech and B.S. Dandapat, (1992), *Magnetohydrodynamic flow of a power-law fluid over a stretching sheet*, International Journal of Non-Linear Mechanics, 27, No 6, 929-936. doi [10.1016/0020-7462\(92\)90045-9](https://doi.org/10.1016/0020-7462(92)90045-9)
- [5] T.C. Chiam, (1995), *Hydromagnetic flow over a surface stretching with a power-law velocity*, International Journal of Engineering Science, 33, No 3, 429-435. doi [10.1016/0020-7225\(94\)00066-S](https://doi.org/10.1016/0020-7225(94)00066-S)
- [6] A. J. Chamkha, (1999), *Hydromagnetic three-dimensional free convection on a vertical stretching surface with heat generation or absorption*, International Journal of Heat and Fluid Flow, 20, No 1, 84-92. doi [10.1016/S0142-727X\(98\)10032-2](https://doi.org/10.1016/S0142-727X(98)10032-2)
- [7] M. Subhas Abel, A. Joshi and R.M. Sonth, (2001), *Heat Transfer in MHD Visco-elastic Fluid Flow over a Stretching Surface*, ZAMM - Journal of Applied Mathematics and Mechanics, 81, No 10, 691-698. doi [10.1002/1521-4001\(200110\)81:10<691::AID-ZAMM691>3.0.CO;2-Z](https://doi.org/10.1002/1521-4001(200110)81:10<691::AID-ZAMM691>3.0.CO;2-Z)
- [8] M. Sheikholeslami, M. Hatami and G. Domairry, (2015), *Numerical simulation of two phase unsteady nanofluid flow and heat transfer between parallel plates in presence of time dependent magnetic field*, Journal of the Taiwan Institute of Chemical Engineers, 46, 43-50. doi [10.1016/j.jtice.2014.09.025](https://doi.org/10.1016/j.jtice.2014.09.025)
- [9] S. Ostrach, (1952), *An analysis of laminar free-convection flow and heat transfer about a flat plate parallel to the direction of the generating body force*, National Advisory Committee for Aeronautics, Document ID: 19930092147, 17 p.
- [10] C. P. Kothandaraman and S. Subramanyan, (2006), *Heat and Mass Transfer Data Book*, New Age International Publishers, New Delhi.
- [11] A. Moutsoglou and T. S. Chen, (1980), *Buoyancy Effects in Boundary Layers on Inclined, Continuous, Moving Sheets*, Journal of Heat Transfer, 102, No 2, 371-373. doi [10.1115/1.3244292](https://doi.org/10.1115/1.3244292)
- [12] K. Vajravelu, (1994), *Convection Heat Transfer at a Stretching Sheet with Suction or Blowing*, Journal of Mathematical Analysis and Applications, 188, No 3, 1002-1011. doi [10.1006/jmaa.1994.1476](https://doi.org/10.1006/jmaa.1994.1476)
- [13] A. Ishak, R. Nazar and I. Pop, (2008), *Hydromagnetic flow and heat transfer adjacent to a stretching vertical sheet*, Heat and Mass Transfer, 44, 921-927. doi [10.1007/s00231-007-0322-z](https://doi.org/10.1007/s00231-007-0322-z)
- [14] M. Ali and F. Al-Yousef, (1998), *Laminar mixed convection from a continuously moving vertical surface with suction or injection*, Heat and Mass Transfer, 33, No 4, 301-306. doi [10.1007/s002310050193](https://doi.org/10.1007/s002310050193)
- [15] R. Nandkeolyar et al., (2013), *Unsteady Hydromagnetic Natural Convection Flow of a Dusty Fluid Past an Impulsively Moving Vertical Plate With Ramped Temperature in the Presence of Thermal Radiation*, Journal of Applied Mechanics, 80, No 6, 9 p. doi [10.1115/1.4023959](https://doi.org/10.1115/1.4023959)
- [16] A. Mastroberardino, (2014), *Mixed Convection in Viscoelastic Boundary Layer Flow and Heat Transfer Over a Stretching Sheet*, Advances in Applied Mathematics and Mechanics, 6, No 3, 359-375. doi [10.4208/aamm.2013.m303](https://doi.org/10.4208/aamm.2013.m303)
- [17] D. Srinivasacharya and Ch. RamReddy, (2011), *Mixed Convection Heat and Mass Transfer in a Micropolar Fluid with Soret and Dufour Effects*, Advances in Applied Mathematics and Mechanics, 3, No 4, 389-400. doi [10.4208/aamm.10-m1038](https://doi.org/10.4208/aamm.10-m1038)
- [18] K.V. Prasad, K. Vajravelu and P.S. Datti, (2010), *The effects of variable fluid properties on the hydro-magnetic flow*

- and heat transfer over a non-linearly stretching sheet, *International Journal of Thermal Sciences*, 49, No 3, 603-610. doi [10.1016/j.ijthermalsci.2009.08.005](https://doi.org/10.1016/j.ijthermalsci.2009.08.005)
- [19] S. Ahmad, N. M. Arifin, R. Nazar, and I. Pop, (2008), *Mixed convection boundary layer flow along vertical moving thin needles with variable heat flux*, *Heat and Mass Transfer*, 44, 473-479. doi [10.1007/s00231-007-0263-6](https://doi.org/10.1007/s00231-007-0263-6)
- [20] F. Talay Akyildiz et al., (2010), *Similarity solutions of the boundary layer equations for a nonlinearly stretching sheet*, *Mathematical Methods in the Applied Sciences*, 33, No 5, 601-606. doi [10.1002/mma.1181](https://doi.org/10.1002/mma.1181)
- [21] P. K. Kameswaran, P. Sibanda, M. K. Partha and P. V. S. N. Murthy, (2014), *Thermophoretic and Nonlinear Convection in Non-Darcy Porous Medium*, *Journal of Heat Transfer*, 136, No 4, 9 p. doi [10.1115/1.4025902](https://doi.org/10.1115/1.4025902)
- [22] L. L. Lee, (1967), *Boundary Layer over a Thin Needle*, *The Physics of Fluids*, 10, No 4, 820-822. doi [10.1063/1.1762194](https://doi.org/10.1063/1.1762194)
- [23] T. Fang, J. Zhang and Y. Zhong, (2012), *Boundary layer flow over a stretching sheet with variable thickness*, *Applied Mathematics and Computation*, 218, No 13, 7241-7252. doi [10.1016/j.amc.2011.12.094](https://doi.org/10.1016/j.amc.2011.12.094)
- [24] M. M. Khader and A. M. Megahed, (2015), *Boundary layer flow due to a stretching sheet with a variable thickness and slip velocity*, *Journal of Applied Mechanics and Technical Physics*, 56, No 2, 241-247. doi [10.1134/S0021894415020091](https://doi.org/10.1134/S0021894415020091)
- [25] K. V. Prasad, K. Vajravelu and H. Vaidya, (2016), *MHD Casson Nanofluid Flow and Heat Transfer at a Stretching Sheet with Variable Thickness*, *Journal of Nanofluids*, 5, No 3, 423-435. doi [10.1166/jon.2016.1228](https://doi.org/10.1166/jon.2016.1228)
- [26] K. Vajravelu, K. V. Prasad, C.-O. Ng and H. Vaidya, (2016), *MHD Flow and Heat Transfer Over a Slender Elastic Permeable Sheet in a Rotating Fluid with Hall Current*, *International Journal of Applied and Computational Mathematics*, 1-26. doi [10.1007/s40819-016-0291-3](https://doi.org/10.1007/s40819-016-0291-3)
- [27] K. Vajravelu, K. V. Prasad and H. Vaidya, (2016), *Influence of Hall Current on MHD Flow and Heat Transfer over a slender stretching sheet in the presence of variable fluid properties*, *Communications in Numerical Analysis*, 1, 17-36. doi [10.5899/2016/cna-00251](https://doi.org/10.5899/2016/cna-00251)
- [28] K. V. Prasad, H. Vaidya, K. Vajravelu and M. M. Rashidi, (2016), *Effects of Variable Fluid Properties on MHD Flow and Heat Transfer over a Stretching Sheet with Variable Thickness*, *Journal of Mechanics*, 33, No 4, 501-512. doi [10.1017/jmech.2016.101](https://doi.org/10.1017/jmech.2016.101)
- [29] I. A. Hassanien, (1997), *The Effect of Variable Viscosity on Flow and Heat Transfer on a Continuous Stretching Surface*, *ZAMM - Journal of Applied Mathematics and Mechanics*, 77, No 11, 876-880. doi [10.1002/zamm.199707711114](https://doi.org/10.1002/zamm.199707711114)
- [30] H. B. Keller, (1993), *Numerical Methods for Two-Point Boundary-Value Problems*, Dover Publications, New York.
- [31] K. Vajravelu and K. V. Prasad, (2014), *Keller-Box Method and Its Application*, Higher Education Press and Walter De Gruyter GmbH, Berlin/Boston.
- [32] L. J. Grubka and K. M. Bobba, (1985), *Heat transfer characteristics of a continuous stretching surface with variable temperature*, *Journal of Heat Transfer*, 107, No 1, 248-250. doi [10.1115/1.3247387](https://doi.org/10.1115/1.3247387)
- [33] C.-H. Chen, (1998), *Laminar mixed convection adjacent to vertical, continuously stretching sheets*, *Heat and Mass Transfer*, 33, No 5-6, 471-476. doi [10.1007/s002310050217](https://doi.org/10.1007/s002310050217)
- [34] M. E. Ali, (1994), *Heat transfer characteristics of a continuous stretching surface*, *Wärme - und Stoffübertragung*, 29, No 4, 227-234. doi [10.1007/BF01539754](https://doi.org/10.1007/BF01539754)

This page is intentionally left blank